ACS Catalysis

Research Article

pubs.acs.org/acscatalysis

Effects of Binders on the Performance of Shaped Hierarchical MFI Zeolites in Methanol-to-Hydrocarbons

Nina-Luisa Michels, Sharon Mitchell, and Javier Pérez-Ramírez*

Institute for Chemical and Bioengineering, Department of Chemistry and Applied Biosciences, ETH Zurich, Vladimir-Prelog-Weg 1, CH-8093 Zurich, Switzerland

Supporting Information

ABSTRACT: The scale-up of zeolite catalysts from powder to industrially relevant shapes is widely neglected in fundamental research because of the added preparative and analytical complexity. Binders incorporated to improve mechanical stability and related structuring steps can cause decisive performance alterations, which are currently difficult to predict. Here, by characterizing physical, extruded, and milled admixtures of MFI zeolites with common silica, alumina, or clay binders, we elucidate the cause and magnitude of property variations induced by shaping. Subsequent evaluation in the conversion of methanol to hydrocarbons confirms the corresponding catalytic impacts. Our findings show that binder effects can, without optimization, match or even exceed those of hierarchically structuring the porosity of the MFI crystals. The macroporosity and related mass transfer properties of the technical bodies are enhanced on extrusion with attapulgite and kaolin as a result of their larger particle size. Comparatively, the acid site density and speciation is binder-dependent. Although a decreased Brønsted acidity, due to the partial dealumination or ion exchange of the zeolite framework, reduces the intrinsic activity of the catalysts, no direct correlation is observed with the selectivity or catalyst lifetime. The unique role of attapulgite in promoting the longevity and light-olefin selectivity of the zeolite is correlated with the reversible neutralization of the framework by mobile Mg species. Ball-milling proves a complementary tool to rapidly screen for potential reactions between component phases with small sample quantities. An improved understanding of the complex morphological and chemical interactions within zeolite−binder composites and of how they can be effectively tuned will ultimately accelerate the development of superior catalytic technologies.

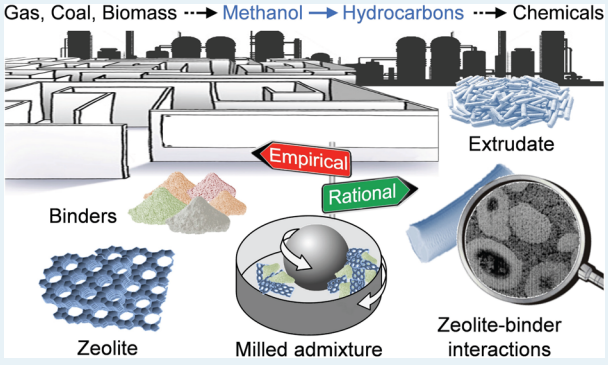

KEYWORDS: *zeolite, catalysis, shaping, binder, methanol-to-hydrocarbons, lifetime, selectivity*

1. INTRODUCTION

The development of industrial catalysts implies the identification of practically and economically scalable recipes to obtain high-performance materials in macroscopic forms suitable for their large-scale implementation.[1,2] Although the approach to scale up, including the choice of formulation and shaping method, can profoundly impact the properties of the resulting catalysts, few academic studies have been devoted to rationalizing the possible effects. The need for a better understanding was recently highlighted in the vibrant area of zeolite catalysis, revealing that interactions with binders, which are vital components for their technical application, could result in multiple effects of both chemical and physical origin.[3,4]

An important zeolite-catalyzed reaction in which binders have been reported influential is the conversion of methanol to hydrocarbons (MTH).[5−13] Significant advancement in the mechanistic understanding of the interplay between the properties, the process conditions, and the performance has been gained over a wide variety of zeolite framework types, including those of the commercially applied ZSM-5 (MFI-type) and SAPO-34 (CHA-type) catalysts.[14−19] However, since the vast majority of this knowledge was derived over pure zeolite powders, the impact of shaping remains intangible.

The potential relevance of zeolite−binder interactions can be clearly illustrated in the case of ZSM-5 catalysts, which exhibit a broad product distribution.[15] Consequently, the zeolite properties must be carefully tuned to optimize the selectivity to the desired product slate. For example, when targeting olefins, the density or strength of the Brønsted acid sites is known to be crucial.[15,16] Moderation of the latter by direct synthesis (e.g., by adjusting the Si/Al ratio[16,20]) or through post-synthetic modification (e.g., by impregnation with diverse species such as P, Ga, B, Ca, Mg etc.,[21−25]) or by dealumination[26] or silylation[27] treatments are all strategies to enhance the performance. Nonetheless, because it is well known that acid sites can be created or lost as a result of the intimate contact between the zeolite and binder phases in shaped catalysts,[6,7,28]

Received: March 18, 2014
Revised: June 8, 2014
Published: June 13, 2014

   dx.doi.org/10.1021/cs500353b | ACS Catal. 2014, 4, 2409−2417

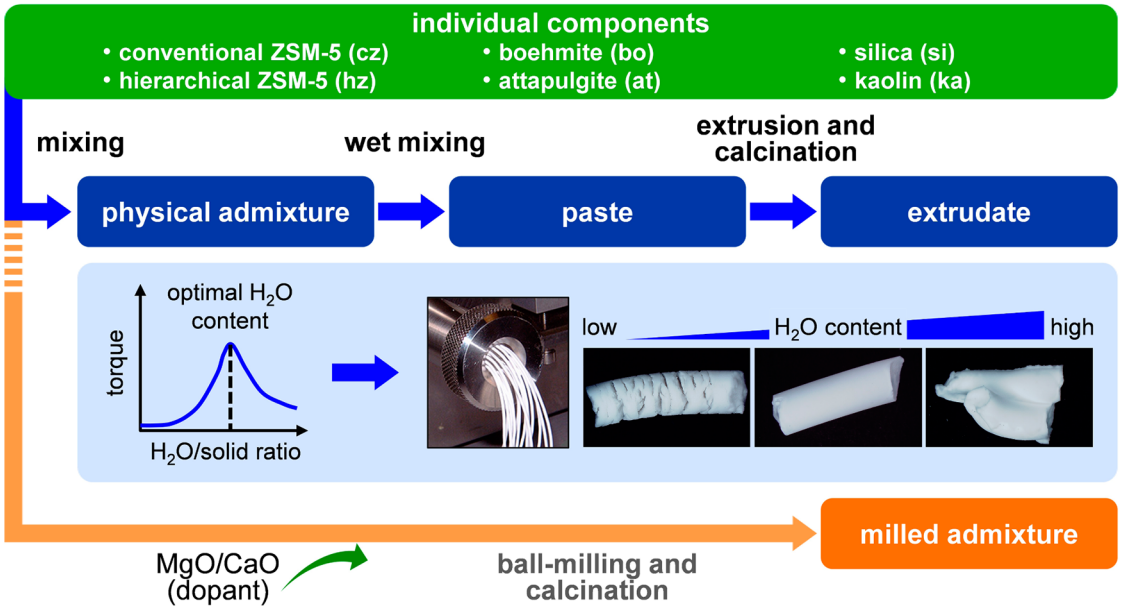

Figure 1. Principal stages in the preparation of zeolite extrudates with various binders (indicated in blue). Ball-milling provides a parallel route by which to maximize zeolite−binder interactions (indicated in orange).

an improved understanding and control over binder effects would be advantageous.

Another critical consideration in the design of MTH catalysts is how to abate the progressive loss of activity due to fouling with time-on-stream, which determines the reactor downtime in the fixed-bed process. A significant advance was the recognition that the coke tolerance can be improved through hierarchically structuring the zeolite porosity.[29−32] This can be achieved either through the introduction of intracrystalline mesopores, (e.g., by carbon-templating[29] or demetalation,[13,30,31]) or through the synthesis of nanosized zeolites (e.g., by organic cotemplating[29]) or by seeded synthesis in fluoride media.[32] Although we recently demonstrated that a superior lifetime could be preserved in technical form,[13] the impact of shaping, either as a result of the change in macroscopic structure or the potential reaction with the binder, on the performance of the hierarchical zeolite was not decoupled.

To provide further insight into binder effects, this manuscript studies the influence of shaping with commercial silica, alumina, kaolin, and attapulgite clay binders on the properties of conventional and hierarchical ZSM-5 zeolite catalysts of different framework compositions. The origin and extent of shaping-induced variations in the porosity and acidity of the catalysts are elucidated by systematic characterization of the individual components and of zeolite−binder admixtures prepared by physical mixing, extrusion, or ball-milling. The impact on the activity, selectivity, lifetime, and coking behavior of the composite catalysts in the MTH reaction is subsequently quantified at different temperature and weight-hourly space velocity. The beneficial application of ball-milling as a parallel lab-scale tool through which to simulate the intimate phase contact experienced during extrusion is demonstrated.

2. EXPERIMENTAL SECTION

2.1. Catalyst Preparation. The hydrothermal synthesis and pilot-scale desilication of the conventional ZSM-5 zeolite (Si/Al = 39, coded **cz40**) to obtain the hierarchical analogue (coded **hz40**) is elaborated elsewhere.[33] The binders investigated in this study included silica (Sipernat 320D, Evonik, coded **si**); acid-dispersed boehmite (0.3 M HNO_3, 3.3 $cm^3\ g_{binder}^{-1}$, Dispersal, Sasol, coded **bo**); and two natural clays, kaolin (Sigma-Aldrich, coded **ka**) and attapulgite (Sigma-Aldrich, coded **at**). Acid-treated attapulgite (coded $\mathbf{at_{HCl}}$) was obtained by treating the as-received clay in aqueous HCl (1 M, 30 $cm^3\ g_{binder}^{-1}$) at 298 K for 1 h, followed by filtration and washing.

The principal steps in the laboratory-scale extrusion of the conventional or hierarchical zeolites are shown in Figure 1. The zeolite and binder (1:1 dry mass ratio, accounting for the weight loss upon calcination to 873 K) were homogenized in a speed mixer (SpeedMixer, FlackTek Inc.), first as dry powders and then in the presence of a predetermined amount of water to form pastes that could be subsequently shaped using a Mini-Screw Extruder (Caleva). A mixer torque rheometer (MTR3, Caleva) was used to optimize the solid-to-liquid ratio. The resulting extrudates were dried in a convection oven (Universal Oven UF, Memmert) for 12 h at 393 K prior to calcination at 873 K for 3 h (2 K min^{-1}) in flowing air (60 $cm^3\ min^{-1}$) in a tubular furnace (Carbolite GHA).

Physical admixtures were obtained by directly mixing the calcined (873 K, 3 h, 2 K min^{-1}, 60 $cm^3\ min^{-1}$ flowing air) zeolite and binder powders (1:1 mass ratio). Milled zeolite−binder admixtures were prepared by treatment in the presence of water (20 vol % more than the amount required for extrusion) using a planetary ball mill (60 min, 500 rpm, Retsch) and were dried and calcined equivalently to the extrudates. In some cases, the zeolite−binder admixtures were doped with MgO (2.5 wt %, Strem Chemicals, coded e.g., $\mathbf{ka_{Mg}}$).

To verify the impact of the framework composition, two additional commercial ZSM-5 zeolites with nominal Si/Al ratios of 15 and 140 (CBV 28014 and CBV 3024E from Zeolyst, both NH_4 form, coded **cz15** and **cz140**, respectively) were compared as reference materials. In this case, the hierarchical ZSM-5 counterparts (coded **hz15** and **hz140**) were obtained by alkaline treatment (338 K, 30 min, 30 $cm^3\ g_{zeolite}^{-1}$) in an aqueous solution of 0.6 M NaOH or 0.3 M

dx.doi.org/10.1021/cs500353b | ACS Catal. 2014, 4, 2409−2417

Table 1. Characterization and Performance Data of the Pure Powder and Extruded Zeolite Catalysts

sample	form[a]	V_{micro}[b] ($cm^3\ g^{-1}$]	S_{meso}[b] ($m^2\ g^{-1}$)	V_{meso}[c] ($cm^3\ g^{-1}$)	V_{macro}[e] ($cm^3\ g^{-1}$)	c_B[f] ($\mu mol\ g^{-1}$)	c_L[f] ($\mu mol\ g^{-1}$)	lifetime[g] (h)	$S(C_{2-4}^{=})$[g] (C mol %)	$S(C_{6-8})$[g] (C mol %)
cz40	P	0.14	82	0.13 (0.04)[d]	na	174	35	20	39	15
hz40	P	0.12	183	0.49 (0.33)	na	212	52	41	40	10
hz40-si	E	0.07	144	0.49 (0.76)	0.15	50	52	12	33	12
hz40-bo	E	0.06	180	0.49 (0.40)	0.10	96	161	21	27	12
hz40-ka	E	0.07	94	0.27 (0.25)	0.29	190	70	52	42	10
hz40-at	E	0.06	159	0.48 (0.44)	0.19	113	185	71	51	5
hz40-at	E[h]	0.06	155	0.46 (0.44)	0.19	93	160	73	51	4

[a]Powder (P) and extrudate (E), zeolite−binder admixtures comprise 1:1 dry mass ratio. [b]*t*-Plot method. [c]$V_{meso} = V_{pore} - V_{micro}$. [d]In parentheses, volume of Hg intruded into pores of 3.7−50 nm diameter. [e]Volume of Hg intruded into pores >50 nm in diameter. [f]Concentration of Brønsted (c_B) or Lewis (c_L) acid sites per gram of zeolite derived from the IR study of adsorbed pyridine. [g]MTH reaction studied at T = 723 K, P = 1 bar, and WHSV = 9.5 $g_{methanol}\ g_{zeolite}^{-1}\ h^{-1}$. [h]Sample regenerated following deactivation to 70% in the MTH reaction.

NaOH + 0.05 M TPABr for **hz15** and **hz140**, respectively, followed by quenching in ice−water, filtration, and washing. The isolated solids were converted to the protonic form by ion exchange with aqueous NH_4NO_3 (0.1 M, 298 K, 100 $cm^3\ g_{zeolite}^{-1}$) in three consecutive steps for 12 h and subsequent calcination (873 K, 3 h, 2 K min^{-1}, 60 $cm^3\ min^{-1}$ air flow).

2.2. Catalyst Characterization. X-ray diffraction (XRD) was measured with a PANalytical X'Pert Pro diffractometer using Ni-filtered Cu Kα radiation (λ = 0.1541 nm). Solid-state ^{27}Al magic-angle spinning nuclear magnetic resonance (MAS NMR) spectra, referenced to $NH_4Al(SO_4)_2{\cdot}12H_2O$, were acquired on a Bruker Avance 400 MHz spectrometer using a spinning speed of 10 kHz, 2048 accumulations, and 90 pulses (2 μs length, 0.25 s recycle decay). X-ray fluorescence spectrometry (XRF) was conducted with an Orbis Micro-XRF analyzer (EDAX) operated with a Rh source at 30 kV. Nitrogen sorption at 77 K was measured in a Quantachrome Quadrasorb-SI analyzer after evacuation of the samples at 573 K for 6 h. Mercury intrusion was carried out in a Micromeritics Autopore IV 9510 instrument (contact angle = 140°, pressure equilibration time = 10 s). Temperature-programmed desorption of NH_3 was carried out in a Micromeritics AutoChem II 2920 (473−873 K, 10 K min^{-1}). Prior to analysis, the samples were degassed (873 K, 3 h, 20 $cm^3\ min^{-1}$ He), and ammonia was adsorbed in three consecutive saturation (10 vol % NH_3 in 20 $cm^3\ min^{-1}$ He, 30 min) and purging (20 $cm^3\ min^{-1}$ He, 1 h) steps at 473 K. Fourier transform infrared spectroscopy of adsorbed pyridine was conducted using a Bruker IFS 66 spectrometer. After evacuation at 673 K for 4 h, wafers of pressed sample were saturated with pyridine vapor, and further evacuated at 473 K for 30 min. Spectra were acquired in the range of 4000−650 cm^{-1} with a nominal resolution of 4 cm^{-1} and the coaddition of 31 scans. The concentrations of Brønsted (c_B) and Lewis (c_L) acid sites were determined from the bands at 1545 and 1445 cm^{-1}, respectively, using extinction coefficients of 1.67 and 2.94 cm μmol^{-1}, respectively.[34] Thermal gravimetric analysis was performed in a Mettler Toledo TGA/SDTA851e microbalance. Focused ion beam scanning electron microscopy of resin-embedded extrudates was performed with a Zeiss NVision 40 instrument using energy-selective backscattered electron detection (2 kV). SEM and TEM images were taken with a Zeiss Gemini 1530 FEG microscope (5 kV) and a FEI Tecnai F30 microscope (300 kV), respectively.

2.3. Diffusion Studies. The adsorption of 2,2-dimethylbutane (>99%, ABCR) was studied in an Intelligent Gravimetric Analyzer (IGA-002, Hiden Isochema). Prior to analysis, the powder or extrudate (~30 mg) was outgassed in situ (573 K, 4 h, 10^{-5} bar). At a desired temperature (338, 348, and 358 K), the sample was subjected to a pressure step (0.1 mbar) of 2,2-dimethylbutane vapor, and the weight change was continuously recorded until equilibrium was reached.

2.4. Methanol-to-Hydrocarbons Testing. The conversion of methanol over the powder (200−400 μm sieve fraction) and extrudate (2 mm in diameter, 4 mm in length) catalysts was evaluated in a Microactivity-Reference unit (PID Eng&Tech) at 623 or 723 K and ambient pressure. The catalysts (0.5 g with respect to the zeolite mass, mixed with 1.5 g SiC of 400−600 μm diameter) were loaded in a fixed-bed, continuous-flow reactor (13.5 mm i.d.) and heated for 1 h at 773 K under a N_2 flow prior to reaction. The temperature was recorded with a thermocouple coaxially positioned in the center of the reactor in contact with the catalyst. Methanol (99.9%, Sigma-Aldrich) was introduced via an HPLC pump (307 5-SC-type piston pump, Gilson) using N_2 as the carrier gas to attain the desired weight hourly space velocity with respect to the zeolite content (9.5 $g_{methanol}\ g_{zeolite}^{-1}\ h^{-1}$ unless otherwise specified). The dependence of conversion, defined as the fraction of light oxygenates (methanol and dimethyl ether) consumed during the reaction on a carbon mole basis (C mol %), on the WHSV was assessed by varying the mass of the catalyst. The product mixture was analyzed by online gas chromatography (GC 7890A, Agilent Technologies) using a HP PLOT Q capillary column and a flame ionization detector. Individual products were identified and lumped together according to retention times established by comparison with pure standards, and carbon balances of between 96 and 99% were usually achieved. Catalyst regeneration was accomplished by flowing air (50 $cm^3\ min^{-1}$) at 823 K for 3 h over the extrudate bed.

3. RESULTS AND DISCUSSION

3.1. Preparation and Characteristics of Technical ZSM-5 Catalysts. Figure 1 illustrates the protocol used to shape conventional (**cz40**) and hierarchical ZSM-5 (**hz40**) powders with one of four commercial binders: (i) an acid-dispersible boehmite (**bo**) with a nominal particle size of 80 nm, (ii) a hydrophilic precipitated silica (**si**) with a nominal agglomerate size of 7.5 μm, (iii) a high-quality attapulgite clay (**at**) with an agglomerate size (as-received) of 30 μm, and (iv) a high-quality kaolin clay (**ka**) of 20 μm particle size. Herein, the greater compositional complexity of the natural clays is noteworthy: semiquantitative analysis by X-ray fluorescence spectroscopy revealed a composition of 17.9 Al_2O_3/53.9 SiO_2/

dx.doi.org/10.1021/cs500353b | ACS Catal. 2014, 4, 2409−2417

14.2 MgO/3.7 P_2O_5/1.1 K_2O/2.6 CaO/0.4 TiO_2/6.1 Fe_2O_3 for attapulgite and 49.1 Al_2O_3/50.3 SiO_2/0.1 TiO_2/0.5 Fe_2O_3 for kaolin, respectively. Detailed characterization of the thermal stability of the binders and of their crystallinity, porosity, acidity, and MTH activity after calcination at 873 K is provided in the Supporting Information (SI) (Figure S1a−e, Table S1). The porous and acidic properties of the conventional and hierarchical ZSM-5 zeolites applied in this study are reported in Table 1. Pertinently, alkaline treatment of **cz40** more than doubled the mesopore surface area in **hz40** and led to an 8-fold increase in the accessible mesopore volume determined by Hg intrusion. On the other hand, the hierarchical sample displayed a slightly enhanced concentration of Brønsted and Lewis acid sites.

The organization of zeolite and binder particles upon agglomeration by extrusion defines an additional interparticle meso−macropore network, which can be quantitatively assessed by mercury intrusion (Figure 2a, Table 1) and

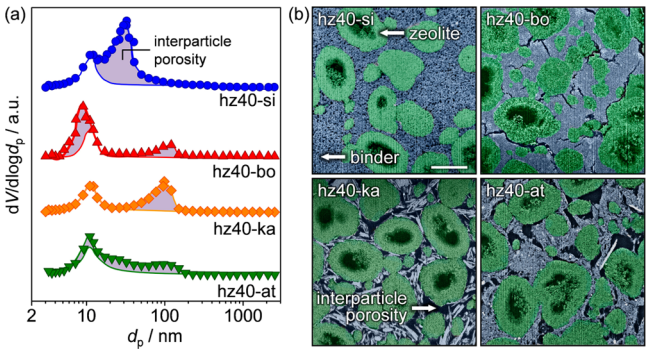

Figure 2. Pore size distributions derived by Hg intrusion of physical (lines) and extruded (symbols) admixtures of the binder and hierarchical ZSM-5 (a). Colored backscattered electron micrographs of FIB-prepared cross-sections of the binder-containing hierarchical ZSM-5 extrudates (b). The scale bar represents 2 μm and applies to all images.

visualized by focused ion beam-scanning electron microscopy (Figure 2b).[11] Densely packed structures, exhibiting the lowest macropore volume and smallest average interparticle pore diameter, resulted upon shaping the hierarchical ZSM-5 with the binders of smallest particle size, for example, the dispersed boehmite. In contrast, structuring with the larger platelike particles of kaolin led to the most open arrangement. Extrusion can induce significant morphological changes in the binders, as can be seen by comparison with the electron micrographs of the single phase powders (SI Figure S1e). For example, the large spherical agglomerates (~30 μm in diameter) observed in the as-received attapulgite powder were dispersed into needlelike nanoparticles wrapped around the zeolite particles in the extrudate. The likelihood of such dispersion could be assessed by laser diffraction analysis of the particle size distribution before and after ultrasonic treatment in water (SI Figure S2).

The adsorption properties of the shaped zeolite catalysts were characterized by measuring the transient uptake curves of 2,2-dimethylbutane at varying temperatures, adopting a methodology recently developed by our group.[35] This probe molecule is ideal for ZSM-5 zeolites because it exhibits a kinetic diameter (0.61 nm) similar to the diameter of an MFI micropore (0.56 nm), decreasing the rate of uptake. In that study, an almost four times higher global diffusivity (D_{global}) was evidenced over the hierarchical with respect to the conventional ZSM-5 powder at 358 K and 0.1 mbar, which was correlated with the additional intracrystalline mesoporosity. Consistent with the proportional contribution of the component phases, a 50% reduction in D_{global} was observed in the physical mixture, resulting upon inclusion of an attapulgite binder **hz40-at**. Moreover, the further drop in the adsorption kinetics from 7.5 × 10^{-20} to 5.3 × 10^{-20} m^2 s^{-1} evidenced upon extrusion is consistent with the longer path length of diffusion within the shaped body. It is known that the mass transfer within shaped zeolite bodies can be dominated by diffusion in the macropores, representing up to 80% of the global mass transfer, particularly at high temperature.[35,36] In fact, a clear dependence on V_{macro} was observed on comparison of the D_{global} determined at 358 K and 0.1 mbar for the conventional and hierarchical ZSM-5 extrudates prepared with different binders (Figure 3).

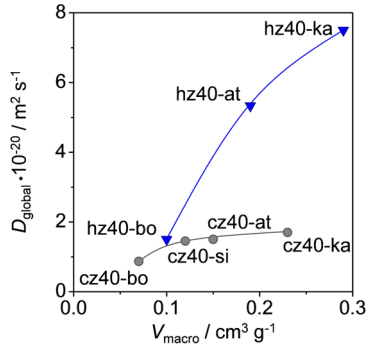

Figure 3. Global diffusion coefficients (D_{global}) of 2,2-dimethylbutane in binder-containing conventional (circles) and hierarchical (triangles) ZSM-5 extrudates as a function of macropore volume at 358 K and 0.1 mbar. The trend lines are drawn for guidance only.

Interestingly, a much larger variation in the adsorption kinetics was observed for the hierarchical zeolite catalysts, suggesting that the effectiveness of the intracrystalline mesopores at enhancing molecular transport is limited by densely packed structures displaying interparticle porosity in the mesopore range.

Finally, evaluation of the acidic properties by the IR study of adsorbed pyridine evidenced reduced concentrations of Brønsted acid sites per gram of zeolite (c_B) in all of the shaped hierarchical ZSM-5 catalysts (Table 1), with **hz40-ka** > **hz40-at** > **hz40-bo** > **hz40-si**. Such losses could arise from either (i) the removal of Brønsted acid sites due to dealumination of the zeolite framework or (ii) their partial neutralization due to the ion exchange with mobile species. For example, the latter has been previously reported in the case of sodium montmorillonite[28] or kaolin clays.[38] To further understand the variation in Brønsted acidity, the samples were further characterized by NH_3-TPD, FTIR, and ^{27}Al MAS NMR, as shown for selected samples in Figure 4a−c. The most prominent drop in c_B, to less than 1/3 of that expected based on the proportional contribution of the zeolite and binder phases, was observed over the silica-bound zeolites. Herein, the decline in the contribution above 700 K in the NH_3-TPD profile, the disappearance of the band at 3600 cm^{-1} in the IR spectrum, and the reduction in the peak intensity associated with tetrahedrally coordinated Al species (54 ppm) in the ^{27}Al MAS NMR spectrum indicated that the loss of Brønsted sites occurred as a result of dealumination of the zeolite framework. Nonetheless, the cause of this effect remains unclear, and few

dx.doi.org/10.1021/cs500353b | ACS Catal. 2014, 4, 2409−2417

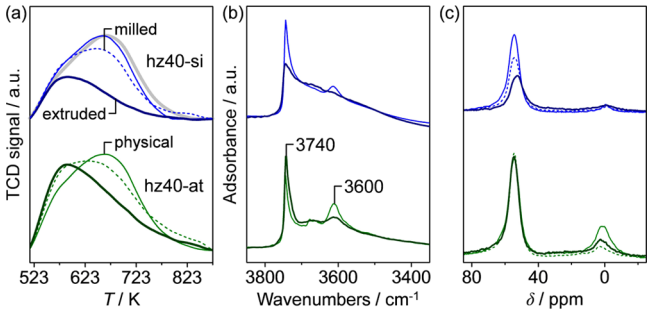

Figure 4. NH_3-TPD profiles (a), FTIR spectra in the OH-stretching region (b), and ^{27}Al MAS NMR spectra (c) of physical (thin line), extruded (thick line), and milled (dashed line) **hz40-si** (top) and **hz40-at** (bottom) admixtures normalized to the zeolite content. The thick gray line in part a indicates the NH_3-TPD profile of the single-phase **hz40** powder.

studies have addressed variations in the acidity of zeolite catalysts when shaped with silica binders.[7] No such impact was observed in the physical mixture of these silica and zeolite phases prepared as a reference. Determination of the origin of the reduced c_B was more complex for **hz40-bo** because of the presence of aluminum in the binder. Previously, this has been linked to the partial neutralization of the Brønsted acid site as a result of the migration of aluminum species from the binder.[7]

Comparatively, the clay binders interacted distinctly with the zeolite. In the case of kaolin, no evidence of a chemical interaction was observed; the acidic properties of **hz40-ka** closely matched those expected on the basis of the characteristics of the pure components. On the other hand, the extruded **hz40-at** exhibited a lower c_B, mirrored by a decrease in the high-temperature contribution in its NH_3-TPD profile and the disappearance of the Brønsted hydroxyl stretch (3600 cm^{-1}) in the FTIR spectra (Figure 4a,b). However, no evidence of dealumination was observed on comparison of the shaped catalyst with respect to the physical mixture of the pure components by ^{27}Al MAS NMR (Figure 4c), suggesting that this loss was due to partial neutralization of the acid sites.

3.2. MTH Performance of Technical Zeolite Catalysts.

The performance of the zeolite extrudates relative to that of the pure powders was evaluated in the conversion of methanol to hydrocarbons at 723 K (Figure 5a) and 623 K (Figure 5b). The mass of the composite catalyst was doubled compared with that of the single-phase materials to achieve an equivalent weight hourly space velocity with respect to the amount of zeolite during initial tests (WHSV = 9.5 $g_{methanol}\ g_{zeolite}^{-1}\ h^{-1}$). The catalyst lifetime, defined as the time for which the conversion of oxygenates (methanol and dimethyl ether) exceeded 90%, and the selectivity to C_{2-4} olefins ($S(C_{2-4}^{=})$) and C_{6-8} aromatics ($S(C_{6-8})$) exhibited at 723 K are summarized in Table 1, and a detailed breakdown of the product distribution is provided in SI Table S2.

Typical of the extensions previously reported over desilicated zeolites,[13,29−31] the hierarchical ZSM-5 powder exhibited a lifetime double that of the conventional zeolite at both temperatures (41 with respect to 20 h, respectively, at 723 K), and only minor differences in selectivity were noted. In comparison, wide variations in both the catalyst lifetime and selectivity were observed over the hierarchical ZSM-5 zeolite upon shaping with different binders, which could not be directly correlated with the porous or acidic properties determined in section 3.1. Extrusion with silica or boehmite

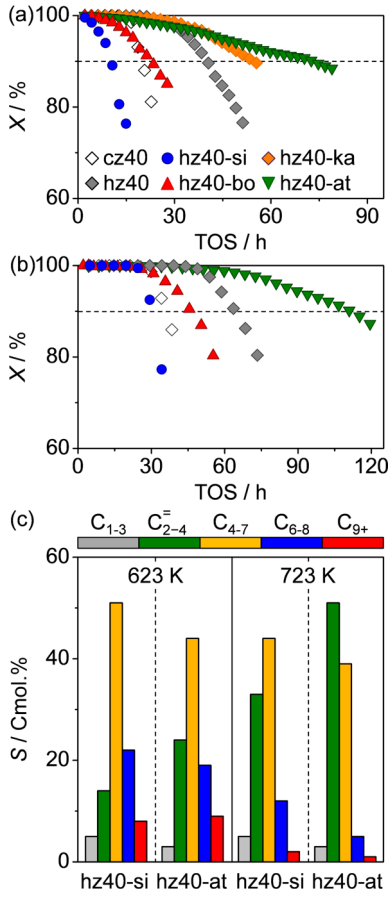

Figure 5. Conversion vs time-on-stream measured at 723 (a) and 623 K (b) and corresponding product selectivities (c) over extruded admixtures of hierarchical ZSM-5 and silica, boehmite, or clay binders. The single-phase conventional (open diamond) and hierarchical (solid diamond) zeolite powders are shown as reference. The dashed line indicates the degree of conversion at which a cycle time was defined. Other conditions: P = 1 bar and WHSV = 9.5 $g_{methanol}\ g_{zeolite}^{-1}\ h^{-1}$.

adversely affected both the catalyst lifetime and selectivity to light olefins while promoting the formation of C_{5-7} hydrocarbons. In the case of **hz40-bo**, a slightly increased production of light gases was consistent with the individual activity of the binder, which catalyzed the formation of CH_4 (SI Table S1). Both the densely packed structures and the sharply reduced Brønsted acidity evidenced in these extrudates could be responsible for these inhibiting effects.

Comparatively, extrusion with kaolin, which induced the smallest deviation in the acidic properties and led to the most open pore structure, did not markedly alter the performance of the hierarchical zeolite. In stark contrast, despite also resulting in a largely reduced Brønsted acidity, the most promising result emerged upon shaping with attapulgite, which led to a 70% increased cycle time and a 25% higher light olefin selectivity (particularly to propene and butenes, SI Table S2) with respect to the pure zeolite. As expected, the main impact of decreasing the temperature was to shift the selectivity from light olefinic to gasoline-range products (Figure 5c), and slower rates of deactivation were also evidenced over all samples. Nonetheless, the binders studied were found to have similar promoting or inhibiting effects at both reaction temperatures. Thus, despite exhibiting the greatest longevity, the **hz40-at** sample retained the highest $C_{2-4}^{=}$ selectivity (>20%) at 623 K.

dx.doi.org/10.1021/cs500353b | ACS Catal. 2014, 4, 2409−2417

Table 2. Characterization and Performance Data of Reference Binder-Containing Hierarchical ZSM-5 Admixtures

sample	form[a]	c_B[b] (μmol g^{-1})	c_L[b] (μmol g^{-1})	lifetime[c] (h)	$S(C_{2-4}^{=})$[c] (C mol %)	$S(C_{6-8})$[c] (C mol %)
$hz40_{Mg}$	M	80	150	65	50	4
hz40-at	M	139	174	80	53	5
hz40-at_{HCl}	M	161	142	57	45	5
hz40-at_{HCl}	PM	195	70	51	41	11
hz40-at_{IE}	M	149	158	70	48	5
hz40-ka	M	145	75	48	41	10
hz40-ka_{Mg}	M	85	189	99	56	4

[a]Milled (M) and physical (PM) zeolite−binder admixtures. [b]Concentration of Brønsted (c_B) or Lewis (c_L) acid sites per gram of zeolite derived from the IR study of adsorbed pyridine. [c]MTH lifetime studied at T = 723 K, P = 1 bar, and WHSV = 9.5 $g_{methanol}\ g_{zeolite}^{-1}\ h^{-1}$.

Further insight into the differing impacts of the binders was obtained by analysis of the intrinsic activity (SI Figure S3) and the coking behavior (SI Figure S4) of the hierarchical zeolite catalysts. Although a similar gradual decrease in the initial conversion was evidenced over the pure **cz40** and **hz40** powders with increasing methanol loading, a much steeper drop was seen over the crushed silica and attapulgite-bound extrudates. This observation is consistent with the lower c_B displayed by these samples and confirms that the 7 times difference in lifetime between **hz40-si** and **hz40-at** cannot be ascribed to a distinct intrinsic activity. Quantification of the coke content of the catalysts after use for a specific time in the MTH reaction revealed that higher amounts were deposited in the samples exhibiting shorter lifetimes. However, the interdependence between coke formation and the lifetime could also not be directly linked to the Brønsted acid site density and corresponding intrinsic activity of the zeolite catalysts. As suggested in section 3.1, this could reflect a different character of acid sites in the binder-containing samples, which may have differing strengths and accessibilities. For example, although Lewis acid sites generated on application of the boehmite binder catalyzed the formation of methane (and coke), which apparently adversely affects the performance of zeolite−alumina composites, no such impact is expected due to the sites that catalyze the dehydration of methanol over the clay binders. Furthermore, the coking behavior is likely to depend on the interplay between multiple parameters. It is known that binders can also be influential during the high-temperature regeneration of shaped zeolites.[37] The reusability of the attapulgite-bound hierarchical ZSM-5 extrudate was confirmed, following oxidative regeneration in air (823 K, 3 h), by the equivalent performance exhibited in the second cycle to the fresh analogue (Table 1).

3.3. Zeolite−Binder Interactions. Several additional steps were taken to distinguish the possible origins (physical or chemical) of the promoting effects evidenced over the MFI catalysts upon shaping with attapulgite. First, the performance of a differently treated **hz40-at** admixture was evaluated to determine under which conditions the property variation occurred (Table 2). Compared with the large extension evidenced over the extruded sample, only a slightly increased cycle time was observed over an **hz40-at** physical mixture with respect to that of the **hz** powder (50 with respect to 41 h, respectively). In contrast, if the **hz40-at** wet paste applied during extrusion was instead ball-milled, a cycle time similar to that of the shaped sample (80 h) resulted. Milling did not adversely impact the crystallinity or the porosity of the zeolite phase. Consistent with the variation observed in the **hz40-at** extrudates, the milled sample exhibited a reduced number of Brønsted coupled with an increased number of Lewis acid sites (Table 2). The comparable behavior of the milled (powder) and extruded samples demonstrates that the promoting effect of the attapulgite binder derives from a chemical interaction with the zeolite and is not significantly impacted by mass transfer effects due to the physical agglomeration of the component phases within the shaped body. In this regard, the application of water or mechanical force (or both) is necessary to induce the property alteration.

As mentioned in section 3.1, the as-received attapulgite contains several species (e.g., Mg, Si, Al, P, K, Ca, Ti, Fe) that could interact with the zeolite (SI Table S3). To further understand their potential effects, both the influence of purifying the attapulgite clay by acid treatment, a typical approach for the removal of soluble metals present in clays,[39] and of doping the kaolin binder with alkaline oxides present in the attapulgite (e.g., MgO) were assessed. Herein, ball-milling was applied as a rapid method to screen for zeolite−binder interactions with smaller sample quantities. Losses of Brønsted acid sites originating as a result of ion exchange should be preventable if the responsible cationic species could be eliminated from the clay binder prior to shaping. Acid treatment of the attapulgite with 1 M HCl solution for 1 h (**at$_{HCl}$**), decreased the concentration of magnesium, and completely removed calcium and phosphorus from the sample (SI Table S3). When milled with the hierarchical ZSM-5, the promoting effect of **at$_{HCl}$** was much less significant than that of **at**, resulting in an MTH lifetime of 57 h with respect to 80 h. Consistently, c_B was less prominently reduced in the milled **hz40-at$_{HCl}$** (Figure 6a), suggesting a considerable decline in the amount of mobile species.

The concept of ion exchange of the Brønsted acid sites could be supported by verifying the reversibility of the interaction.[28] Accordingly, we re-exchanged the milled **hz40-at** admixture by treatment with ammonium nitrate, which decreased the MTH lifetime from 80 to 70 h over **hz40-at$_{IE}$**, further corroborating the link with the exchangeable cations. The strongest evidence for the identity of the responsible mobile species was gained by slowly flushing water through a vertical column filled with phase-separated attapulgite (top) and hierarchical ZSM-5 (bottom). This permitted the water-mediated migration of soluble ions from the binder to the zeolite without their direct contact. XRF analysis revealed the introduction of a significant amount of magnesium into **hz40** after the treatment (SI Table S2).

Assuming that the promoting action of the attapulgite binder on the MTH performance of ZSM-5 zeolites originates from the neutralization of Brønsted acid sites due to exchange with Mg^{2+}, we expected that this result could be extrapolated to other systems. To test this hypothesis, we milled wet MgO-doped admixtures of the kaolin and hierarchical ZSM-5 (Figure

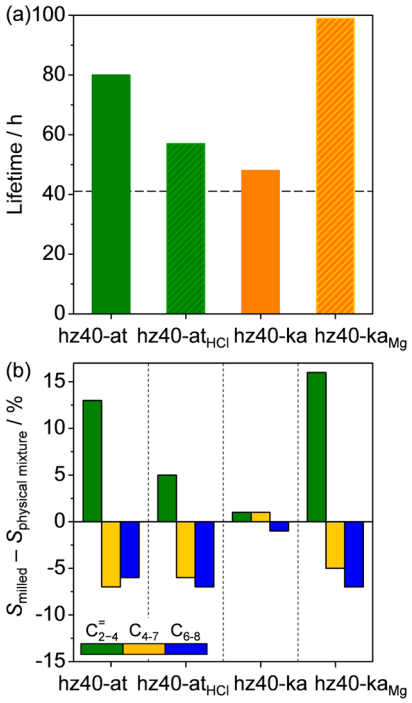

Figure 6. MTH lifetime over milled hierarchical ZSM-5 admixtures with attapulgite, HCl-treated attapulgite, kaolin, and MgO-doped kaolin (a), and the difference in average product selectivity with respect to the corresponding physical mixtures (b). The lifetime of the single-phase hierarchical ZSM-5 powder is indicated by the dashed line in part a. Conditions: T = 723 K, P = 1 bar, and WHSV = 9.5 $g_{methanol}$ $g_{zeolite}^{-1}$ h^{-1}.

6a). No major lifetime enhancement was previously evidenced over the **hz40-ka** extrudate with respect to that observed over the pure hierarchical zeolite (vide supra). As a reference, the milled **hz40-ka** admixture was found to exhibit a lifetime equivalent to that of its physically mixed analogue (48 h), confirming that the ball-milling itself did not alter the catalytic performance. Strikingly, the addition of MgO more than doubled the cycle time (~100 h) with respect to the milled **hz40-ka**, which is consistent with the reduced Brønsted and increased Lewis acid site density exhibited by this sample (Table 2). Comparison of the average product distribution of the milled **hz40-ka$_{Mg}$** evidenced a similar substantial increase of up to 56% in light olefin selectivity, as previously observed in the attapulgite-containing zeolite catalysts (Figure 6b). Moreover, a similar behavior in catalyst lifetime and selectivity was observed over the hierarchical ZSM-5 powder when doped with MgO (Table 2), consistent with its expected promoting role. Prior studies have reported an enhanced olefin selectivity over MgO-modified ZSM-5 zeolites in the MTH reaction.[24,25]

Finally, we attempted to rationalize the impact of zeolite−binder interactions of both physical and chemical origin on the MTH performance over all physical, extruded, and milled hierarchical ZSM-5 admixtures tested. Analysis of the MTH lifetime as a function of the Brønsted acidity (SI Figure S5a) revealed two distinct behaviors resulting from zeolite−binder interactions: (i) that an improved coke tolerance and light olefin selectivity could be achieved through the partial and reversible neutralization of Brønsted acid sites through the migration of soluble alkaline oxide species present in clay binders, and (ii) that thermally or mechanically induced dealumination of the zeolite framework appears to be detrimental to the performance, reducing the cycle time significantly. In the first case, the promoting effects observed over kaolin-containing zeolite catalysts before and after MgO-doping (SI Figure S5b), demonstrate that performance enhancements are achievable by solely varying the zeolite acidity because the porous properties were unaltered. However, in the second case, the possible contributions of porosity cannot be completely neglected because these samples correspond to the catalysts shaped with boehmite and silica binders, the densely packed structures of which could also contribute to the higher amounts of coke formed and shorter MTH lifetimes.

3.4. Interplay between Composition, Zeolite Mesoporosity, and Binder Effects. It is well known that in addition to the influence of porosity, the MTH lifetimes of single phase ZSM-5 zeolites depends on the Si/Al ratio of the framework and, consequently, the relative concentration of Brønsted acid sites.[15,16,20] The latter could also impact the interaction of the zeolite with binders applied during shaping. To generalize the significance of the performance benefits that we had observed upon both mesoporosity introduction and shaping the ZSM-5 zeolite with the attapulgite binder, we verified the potential impact of varying the zeolite composition. For this purpose, ZSM-5 zeolites with nominal Si/Al ratios of 15 and 140 (**cz15** and **cz140**, respectively) and their hierarchical analogues (**hz15** and **hz140**, respectively) obtained by desilication as well as the corresponding attapulgite-bound extrudates (e.g., **hz15-at**) were tested in the MTH reaction at WHSV of 4.8 $g_{methanol}$ $g_{zeolite}$ h^{-1}. It is noteworthy that the comparative evaluation at the higher WHSV (9.5 $g_{methanol}$ $g_{zeolite}$ h^{-1}) applied in the previous section was not possible because complete conversion was not achieved over the high-silica zeolite catalysts under those conditions. Nonetheless, a 9-fold extended MTH lifetime was observed over the conventional ZSM-5 when increasing the Si/Al from 15 to 140 (12 vs 109 h, respectively).

Interestingly, the lifetime enhancement evidenced over the series of hierarchical analogues **hz15**, **hz40**, and **hz140** was reduced with an increase in the Si/Al ratio from 3 to 2.4 to 1.2 times, respectively, suggesting that the effectiveness of mesoporosity development in MTH is lower in the case of high-silica zeolites (Figure 7a). Since both **hz140** and **hz40** possess almost equivalent porous properties (SI Table S4), the different resistance to deactivation appears to be more strongly related to the relative acidity of the conventional and hierarchical zeolites (Table 1, SI S4), and related activity.

Extrusion with attapulgite further increased the MTH lifetime of **hz15-at** with respect to **hz15** by a factor of 1.8, in agreement with the enhancement achieved over **hz40-at** (vide supra). However, a similar promoting effect was not observed in the case of Si/Al = 140, significantly reducing the lifetime of **hz140-at** with respect to **hz140**. As expected, both **hz15-at** and **hz140-at** exhibited a diminished c_B relative to their respective powder analogues, (SI Table S4). However, although the zeolite−binder interaction proved beneficial for the Al-rich **hz15-at**, the density of acid sites was reduced so considerably in **hz140-at** that a catalyst lifetime of only 46 h was reached.

The initial light olefin selectivity was found to increase with varying Si/Al, consistent with a moderation in acid sites due to less aluminum in the zeolite framework (Figure 7b). Furthermore, although mesoporosity introduction exhibited only a very moderate improvement, binding **hz15** with attapulgite more than doubled the C_{2-4} olefin selectivity.

dx.doi.org/10.1021/cs500353b | ACS Catal. 2014, 4, 2409−2417

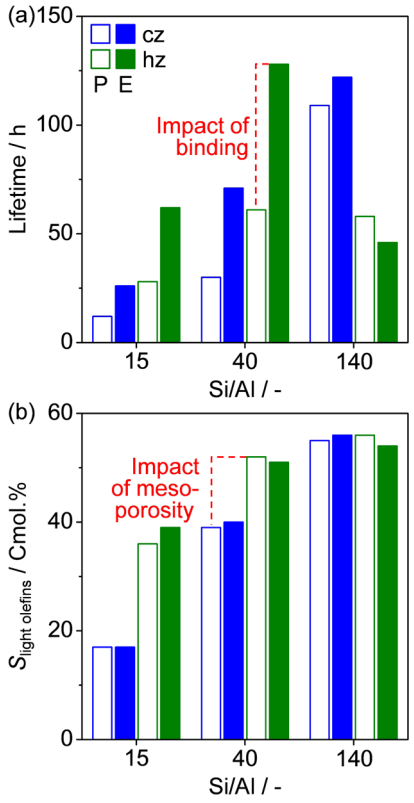

Figure 7. MTH lifetime (a) and average light olefin selectivity (b) evidenced over conventional ZSM-5 zeolite powders of different Si/Al ratio with respect to their hierarchical analogues and to the attapulgite-bound counterparts. Conditions: T = 723 K, P = 1 bar, and WHSV = 4.8 $g_{methanol}\ g_{zeolite}^{-1}\ h^{-1}$.

Interestingly, this effect became less significant with increasing Si/Al, reaching a plateau at ∼60% over **hz140-at**.

It is worth mentioning that the longest lifetime extensions observed at higher methanol loadings (e.g., 99 h over **hz40-ka$_{Mg}$**; vide supra) put the binder-containing hierarchical zeolites in the same range as the high-silica zeolites in terms of cycle times while enabling twice the productivity. Consequently, the introduction of intracrystalline mesoporosity needs to be coupled with the optimization of binder selection to maximize lifetime and, thus, product yield, since both can give substantial improvements. Increasing the Si/Al ratio of the zeolite phase can also extend the cycle time but at the expense of the productivity.

4. CONCLUSIONS

Through systematic comparison of the individual components, and of physical, extruded, and milled zeolite−binder composites, we have demonstrated the significant impact binders can have on the methanol-to-hydrocarbons performance of shaped hierarchical ZSM-5 zeolites. As revealed by Hg porosimetry, the microscopic examination of internal cross-sections, and the gravimetric uptake of 2,2-dimethylbutane, the interaction of the larger particles of the clay binders yields technical bodies exhibiting superior macroporosity and mass transfer properties. Comparatively, distinct variations in the acid site density and speciation were evidenced by spectroscopic and temperature-programmed studies, depending on the binder applied. Although a decreased Brønsted acidity due to the reversible neutralization or dealumination of the zeolite framework reduced the intrinsic activity of the catalysts, no direct correlation was observed with the selectivity or the catalyst lifetime. Without optimization, our findings show that the combined chemical and physical effects of binders can match or even exceed those established on application of hierarchically structured zeolites featuring intracrystalline mesopores and should be considered from the start of the catalyst development program. Attapulgite was the only binder that promoted the longevity and light olefin selectivity of the MFI catalysts, which was linked to the partial ion exchange with mobile Mg species. In contrast, extrusion with silica or boehmite adversely affected the performance of the zeolites. Ball-milling was demonstrated as a complementary tool, enabling the accelerated screening of chemical interactions between the zeolite and binder at bench scale without the need for shaping. The identification of compositional and structural performance descriptors to selectively tune complex zeolite−binder interactions will enable more effective utilization of the diverse properties of these composite catalysts.

■ ASSOCIATED CONTENT

Supporting Information

Characterization and performance data of the binders; an assessment of the particle size of the individual components by laser diffraction; a detailed breakdown of the average MTH selectivity observed over the samples reported in Table 1; the dependence of MTH conversion on WHSV, the coking behavior and the effect of Brønsted acidity and mesoporosity on the catalyst lifetime for selected samples; detailed chemical analysis of reference samples to elucidate the promoting role of the attapulgite binder; characterization and performance data of pure powder and attapulgite-bound zeolites catalysts of varying Si/Al. This material is available free of charge via the Internet at http://pubs.acs.org.

■ AUTHOR INFORMATION

Corresponding Author

*Phone: +41-44-633-7120. E-mail: jpr@chem.ethz.ch.

Notes

The authors declare no competing financial interest.

■ ACKNOWLEDGMENTS

Financial support by the Swiss National Science Foundation (project no. 200021−134572) is acknowledged. M. Milina is thanked for conducting the diffusion studies. Zeochem AG, Uetikon, Switzerland, and the Scientific Center for Optical and Electron Microscopy (ScopeM) at ETH Zurich are thanked for use of their facilities.

■ REFERENCES

(1) Stiles, A. B.; Koch, T. A. *Catalyst Manufacture*; Marcel Dekker Inc.: New York, 1995.

(2) Schüth, F.; Hesse, M. In *Handbook of Heterogeneous Catalysis*; Ertl, G., Knözinger, H., Weitkamp, J., Eds.; Wiley-VCH: Weinheim, Germany, 2008, Vol. *1*, Chapter 2.

(3) Hargreaves, J. S. J.; Munnoch, A. L. *Catal. Sci. Technol.* **2013**, *3*, 1165−1171.

(4) Mitchell, S.; Michels, N.-L.; Pérez-Ramírez, J. *Chem. Soc. Rev.* **2013**, *42*, 6094−6112.

(5) Hölderich, W.; Einhorn, H.; Lehnert, R.; Marosi, L.; Mross, W.; Reinke, R.; Ruppel, W.; Schlimper, H. In *Proceedings of the Sixth International Zeolite Conference*; Olson, D., Bisio, A., Eds.; Butterworths: Reno, NV, USA, 1983; p 545.

(6) Shihabi, D. S.; Garwood, W. E.; Chu, P.; Miale, J. N.; Lago, R. M.; Chu, C. T.-W.; Chang, C. D. *J. Catal.* **1985**, *93*, 471−474.
(7) Martin, A.; Berndt, H.; Lohse, U.; Wolf, U. *J. Chem. Soc., Faraday Trans.* **1993**, *89*, 1277−1282.
(8) Howden, M. G.; Müller, W. P. *Stud. Surf. Sci. Catal.* **1994**, *84*, 1739−1747.
(9) Patcas, F.-C. *J. Catal.* **2005**, *231*, 194−200.
(10) Freiding, J.; Patcas, F.-C.; Kraushaar-Czarnetzki, B. *Appl. Catal., A* **2007**, *328*, 210−218.
(11) Lee, K.-Y.; Lee, H.-K.; Ihm, S.-K. *Top. Catal.* **2010**, *53*, 247−253.
(12) Freiding, J.; Kraushaar-Czarnetzki, B. *Appl. Catal., A* **2011**, *391*, 254−260.
(13) Mitchell, S.; Michels, N.-L.; Kunze, K.; Pérez-Ramírez, J. *Nat. Chem.* **2012**, *4*, 825−831.
(14) Dahl, I. M.; Kolboe, S. *Catal. Lett.* **1993**, *20*, 329−336.
(15) Olsbye, U.; Svelle, S.; Bjørgen, M.; Beato, P.; Janssens, T. V. W.; Joensen, F.; Bordiga, S.; Lillerud, K. P. *Angew. Chem., Int. Ed.* **2012**, *51*, 5810−5831.
(16) Chang, C. D.; Chu, C. T.-W.; Socha, R. F. *J. Catal.* **1984**, *86*, 289−296.
(17) Dessau, R. M. *J. Catal.* **1986**, *99*, 111−116.
(18) Svelle, S.; Joensen, F.; Nerlov, J.; Olsbye, U.; Lillerud, K.-P.; Kolboe, S.; Bjørgen, M. *J. Am. Chem. Soc.* **2006**, *128*, 14770−14771.
(19) Bjørgen, M.; Svelle, S.; Joensen, F.; Nerlov, J.; Kolboe, S.; Bonino, F.; Palumbo, L.; Bordiga, S.; Olsbye, U. *J. Catal.* **2007**, *249*, 195−207.
(20) Howden, M. G.; Botha, J. J. C.; Scurrell, M. S. *Chem. Ind.* **1992**, *46*, 391−407.
(21) Romannikov, V. N.; Chumachenko, L. S.; Mastikhin, V. M.; Ione, K. G. *React. Kinet. Catal. Lett.* **1985**, *29*, 85−91.
(22) Dyaballa, M.; Klemm, E.; Weitkamp, J.; Hunger, M. *Chem. Ing. Tech.* **2013**, *85*, 1719−1725.
(23) Mentzel, U. V.; Højholt, K. T.; Holm, M. S.; Fehrmann, R.; Beato, P. *Appl. Catal., A* **2012**, *417*−*418*, 290−297.
(24) McIntosh, R. J.; Seddon, D. *Appl. Catal.* **1983**, *6*, 307−314.
(25) Lévesque, P.; Bianchi, D.; Le Van Mao, R.; Pajonk, G. M. *Appl. Catal.* **1990**, *57*, 31−43.
(26) Aramburo, L. R.; de Smit, E.; Arstad, B.; van Schooneveld, M. M.; Sommer, L.; Juhin, A.; Yokosawa, T.; Zandbergen, H. W.; Olsbye, U.; de Groot, F. M. F.; Weckhuysen, B. M. *Angew. Chem., Int. Ed.* **2012**, *51*, 3616−3619.
(27) Tynjälä, P.; Pakkanen, T. T. *J. Mol. Catal. A: Chem.* **1997**, *122*, 159−168.
(28) Uguina, M. A.; Sotelo, J. L.; Serrano, D. P. *Appl. Catal.* **1991**, *76*, 183−198.
(29) Kim, J.; Choi, M.; Ryoo, R. *J. Catal.* **2010**, *269*, 219−228.
(30) Bjørgen, M.; Joensen, F.; Holm, M. S.; Olsbye, U.; Lillerud, K.-P.; Svelle, S. *Appl. Catal., A* **2008**, *345*, 43−50.
(31) Vennestrøm, P. N. R.; Grill, M.; Kustova, M.; Egeblad, K.; Lundegaard, L. E.; Joensen, F.; Christensen, C. H.; Beato, P. *Catal. Today* **2011**, *168*, 71−79.
(32) Qin, Z.; Lakiss, L.; Tosheva, L.; Gilson, J.-P.; Vicente, A.; Fernandez, C.; Valtchev, V. *Adv. Funct. Mater.* **2014**, *24*, 257−264.
(33) Pérez-Ramírez, J.; Mitchell, S.; Verboekend, D.; Milina, M.; Michels, N.-L.; Krumeich, F.; Marti, N.; Erdmann, M. *ChemCatChem* **2011**, *3*, 1731−1734.
(34) Emeis, C. A. *J. Catal.* **1993**, *141*, 347−354.
(35) Gueudré, L.; Milina, M.; Mitchell, S.; Pérez-Ramírez, J. *Adv. Funct. Mater.* **2014**, *24*, 209−219.
(36) Chmelik, C.; Kärger, J. *Chem. Soc. Rev.* **2010**, *39*, 4864−4884.
(37) Corma, A.; Grande, M.; Fornés, V.; Cartlidge, S.; Shatlock, M. P. *Appl. Catal.* **1990**, *66*, 45−57.
(38) Choudhary, V. R.; Devadas, E.; Kinage, A. K.; Guisnet, M. *Appl. Catal., A* **1997**, *162*, 223−233.
(39) Suárez Barrios, M.; Flores González, L. V.; Vincente Rodríguez, M. A.; Martín Pozas, J. M. *Appl. Clay Sci.* **1995**, *10*, 247−258.